Geometric Structure of $X(AuPH_3)_4^+$ (X = N, P, As, Sb): T_d or C_{4v}?

Hua Fang and Shu-Guang Wang*

School of Chemistry and Chemical Technology, Shanghai Jiao Tong University, Shanghai 200240, China

Received: July 22, 2006; In Final Form: December 29, 2006

The geometric structures of $X(AuPH_3)_4^+$ (X = N, P, As, Sb) compounds have been determined by DFT and ab-initio methods. In agreement with experiment, $N(AuPH_3)_4^+$ is T_d and $As(AuPH_3)_4^+$ is C_{4v} with an apical As atom. Calculated molecular and experimental crystal structure parameters are compared. The structures of $X(AuPH_3)_4^+$ (X = P, Sb) are predicted. $P(AuPH_3)_4^+$ favors T_d, as confirmed by CC2. The closed-shell interaction distances of Au···Au from Xα are consistent with the experimental values. The electronic structures and chemical deformation densities are analyzed.

1. Introduction

An apparent attraction between two or more nominally monovalent Au(I) ions in cluster compounds has been known for a long time. Typical Au(I)···Au(I) distances are in the range of 300−360 pm. In some cases, the strengths of the Au···Au interactions have been measured by NMR spectroscopy to be in the range of 29−46 kJ/mol, comparable to strong hydrogen bonds. Many theoretical calculations support these data.[1] Schmidbaur coined the name "aurophilic attraction" for this phenonmenon.[2]

This attraction can be strong enough to entirely change the structure of four-coordinate Au(I) complexes. The classical tetrahedral structure in these four-coordinate compounds is abandoned in favor of a square-pyramidal structure once the radius of the central element is too large to allow for short metal−metal bonding in tetrahedral symmetry.[3] While the "gilded ammonium" ion $N(AuPR_3)_4^+$ is approximately tetrahedral in the solid state (R = Ph)[4] as well as for molecules (MP2 calculations, R = H),[5] the valence isoelectronic $As(AuPH_3)_4^+$ was found to form a tetragonal pyramid both in the solid state[3] and in MP2 calculations.[5] Thus, the aurophilicity between the Au(I) atoms can be strong enough to override the tendency of the central atom to form a tetrahedron.

Pyykkö et al.[5] using the MP2 method earlier studied $X(AuL)_4^+$ (X = N, P, As) and reproduced the experimental T_d structure for $N(AuL)_4^+$ and the C_{4v} structure for $As(AuL)_4^+$. C_{4v} was predicted for $P(AuL)_4^+$. However, the at-that-time applied LANL1DZ procedure comprises large-core pseudopotentials and rather small basis sets, and the structures were not fully optimized. It is now known that the Au closed-shell interaction is exaggerated thereby.[6−8] With the Stuttgart[9] small-core pseudorelativistic effective core potentials (ECP) and extended 2f polarization basis sets, Pyykkö et al. reinvestigated the $X(AuL)_4^+$ (X = N, P) systems in 1998.[10] At the MP2 level, $P(AuL)_4^+$ still preferred the C_{4v} structure.

For aurophilic interaction systems, where dispersion interaction plays an important role, it was thought that DF methods are not applicable. However, there is now much evidence that a careful choice of the DF gives reasonable bond lengths and bond energies of Au(I) cluster systems.[11] Therefore, we have here investigated the equilibrium structures and electronic properties of $X(AuPPh_3)_4^+$ (X = N, P, As, Sb) systems, using different DFs, extended basis sets, and fully optimized structures.

2. Computational Details

The structures were fully optimized by DFT, HF, and MP2 methods. The calculations were performed using the Amsterdam density functional package (ADF 2004) initially developed by Baerends et al.[12] and the TURBOMOLE-5.6 package developed by Ahlrichs et al.[13] Four different exchange-correlation DFs were applied: (1) the simple local Xα exchange potential;[14−16] (2) the local correlation-corrected version developed by Vosko, Wilk, and Nusair in 1980[17] with the nonlocal gradient-corrected exchange potential of Becke of 1988[18] and with the nonlocal gradient-corrected correlation potential of Perdew of 1986,[19] here called VBP; (3) Becke's three-parameter (B3) mixture of nonlocal Hartree−Fock exchange and LYP DF exchange-correlation, that is, the B3-LYP-hybrid.[20,21]

In order to reduce the calculational expenses, the inner core shells were frozen,[22] namely, $[1s^2]$ for N, $[1s^2\text{-}2p^6]$ for P, $[1s^2\text{-}3d^{10}]$ for As, $[1s^2\text{-}4d^{10}]$ for Sb, and $[1s^2\text{-}4f^{14}]$ for Au. The atomic core orbitals were calculated by the Dirac method and then kept unrelaxed in the molecules.

Relativistic effects are particularly important for gold and the aurophilic interactions. For DF calculations, we used the scalar relativistic zeroth-order regular approximation (ZORA)[23−27] which averages over spin−orbit splittings. Spin−orbit effects are expected to be unimportant to Au (I) systems.

High-quality triple-ξ plus two polarization basis sets STO-TZ2P were used for the valence shells of all atoms in DFT calculations. In the ab-initio pseudopotential calculations, the qualified GTO-TZVP basis sets from Stuttgart[9] were used for all atoms. The Stuttgart small-core pseudorelativistic effective core potentials (ECP) were selected, which is important concerning Au. The TZVP basis of Au was augmented with two f-type polarization functions (α_f = 0.2, 1.19).[6]

The ligands L of the experimentally studied $X(AuL)_4^+$ (X = N, P, As, Sb) compounds are typically triphenylphosphine $P(C_6H_5)_3$. For computational simplification, it was here replaced by PH_3. This substitution has been found to have little influence on the X−Au and Au−P bond lengths.[28] Models of $X(AuPPh_3)_4^+$ (in T_d or C_{4v}, X = N, P, As, Sb) used in our study are displayed in Figure 1.

* Corresponding author. E-mail: sgwang@sjtu.edu.cn.

10.1021/jp064656b CCC: $37.00
Published on Web 02/07/2007

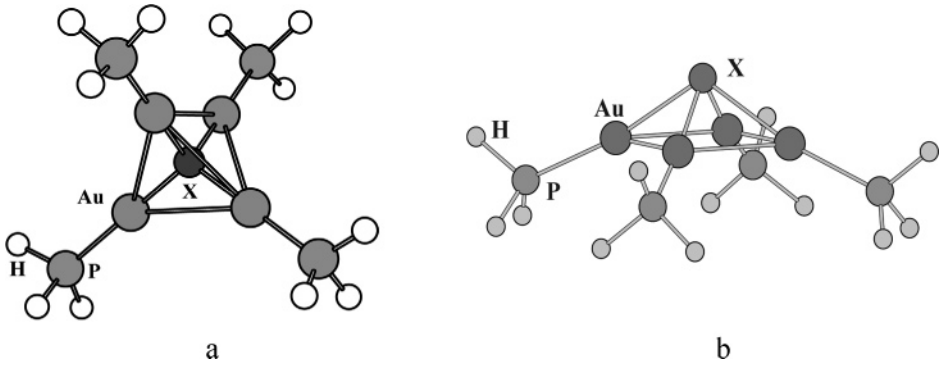

Figure 1. (a) T_d and (b) C_{4v} structures of $X(AuPH_3)_4^+$ (X = N, P, As, Sb).

TABLE 1: Main Geometric Parameters of $X(AuL)_4^+$, X = N(T_d) and As(C_{4v}) (Bond Lengths *R* in pm, and Bond Angles θ in Degrees)

system	method	$R_{Au\cdots Au}$	R_{Au-X}	R_{Au-P}	$\theta_{Au-X-Au}$
$N(AuPH_3)_4^+$	HF	336.4	206.0	235.7	109.5
	MP2	322.7	197.6	225.1	109.5
	Xα	329.0	201.9	224.0	109.5
	VBP	333.4	204.2	224.7	109.5
	B3LYP	333.0	204.4	229.0	109.5
	HF[a]	336.5	206.0	235.2	109.5
	MP2[a]	323.4	198.1	227.1	109.5
	expt[b]	328.6	201.6		
$As(AuPH_3)_4^+$	HF	316.5	255.6	244.6	76.5
	MP2	278.1	248.4	230.8	68.1
	Xα	290.0	254.4	230.0	69.5
	VBP	293.5	255.3	229.9	69.6
	B3LYP	301.0	253.3	236.0	
	HF[c]	306.1	258.6		72.6
	MP2[c]	296.1	260.9		69.1
	expt[d]	290.0	250.0		70.7

[a] HF and MP2 structural values with large basis set from ref 10. [b] Experimental data from refs 3 and 4 for $N(AuPPh_3)_4^+F^-$ crystals. [c] HF and MP2 structural values with small basis set from ref 5. [d] Experimental data from ref 3 for $As(AuPPh_3)_4^+BF_4^-$ crystals.

TABLE 2: Main Geometric Parameters of XAu_4^+ (X = N, P, As, Sb) at Xα/TZ2P Level (Bond Lengths *R* in pm, and Bond Angles θ in Degrees)

system	sym.	$R_{Au\cdots Au}$	$R_{Au}-X$	$\theta_{Au}-X-Au$
NAu_4^+	T_d	318.8	195.3	109.5
	C_{4v}	266.0	206.0	79.9
PAu_4^+	T_d	357.0	218.8	109.5
	C_{4v}	273.1	231.4	72.3
$AsAu_4^+$	T_d	382.0	234.4	109.5
	C_{4v}	273.0	246.8	67.2
$SbAu_4^+$	T_d	408.0	250.2	109.5
	C_{4v}	271.0	261.0	62.7

TABLE 3: Main Geometric Parameters of $X(AuPH_3)_4^+$ (X = N, P, As, Sb) at Xα/TZ2P Level (Bond Lengths *R* in pm, and Bond Angles θ in Degrees)

system	sym.	$R_{Au\cdots Au}$	$R_{Au}-X$	$R_{Au}-P$	$\theta_{Au}-X-Au$
$N(AuPH_3)_4^+$	T_d	329.0	201.9	224.0	109.5
	C_{4v}	283.0	203.4	221.0	88.4
	expt[a]	328.6	201.6		
$P(AuPH_3)_4^+$	T_d	375.0	229.6	227.7	109.5
	C_{4v}	283.4	238.5	225.9	72.9
$As(AuPH_3)_4^+$	T_d	398.0	243.9	225.0	109.5
	C_{4v}	290.0	254.4	230.0	69.5
	expt[b]	290.0	250.0		70.7
$SbAuPH_3)_4^+$	T_d	423.0	259.2	228.0	109.5
	C_{4v}	288.0	268.4	227.0	65.1

[a] Experimental crystal data from refs 3 and 4. [b] Experimental crystal data from ref 4.

3. Results and Discussions

3.1. Structures. *3.1.1. Structures of $N(AuPH_3)_4^+$ (T_d) and $As(AuPH_3)_4^+$ (C_{4v}).* The T_d structure for $N(AuL)_4^+$ [3, 4] and the C_{4v} structure for $As(AuL)_4^+$[4] have been obtained experimentally. The fully optimized structures of the molecular ions from HF, MP2, and DF methods are compared with experimental values of the respective counterion crystals in Table 1. Pyykkö et al. had studied[5,10] $N(AuL)_4^+$ (T_d) at the HF and MP2 levels. HF gives Au···Au distances still too long by about 8 pm when using a qualified basis set. With augmented basis sets, MP2 underestimated the distance by 6 pm. We verified these results. The Xα local density functional applied here reproduced the Au···Au and Au−X bond lengths and Au−X−Au bond angles at best, within a picometer. When nonlocal exchange and correlation correction were added, the Au···Au distance increased by 4 pm (VBP). B3-LYP also significantly overestimated the bond lengths by 5 pm.

As mentioned, Pyykkö et al. had originally studied $As(AuPH_3)_4^+$ (C_{4v}) with small basis sets at the HF and MP2 levels.[5] When the basis set is enlarged, HF gives even longer Au···Au distances, large by about 27 pm, and with the correlation corrections by MP2, the Au···Au distance is underestimated by about 12 pm. The Xα local density functional again reproduced the structural parameters quite well. And again, when nonlocal exchange and correlation corrections are added, the Au···Au distance increased by more than 5 pm (VBP). B3-LYP also significantly overestimated the Au···Au distance (11 pm). So we think that Xα is the most suitable method for investigating these closed-shell systems. On the other hand, MP2 is insufficient for these systems, as concluded already by O'Grady et al.[29] and Pyykkö et al.[30]

3.1.2. Structures of XAu_4^+ and $X(AuPH_3)_4^+$ (X = N, P, As, Sb). It has been found that the classical tetrahedral structure in these four-coordinate compounds is abandoned in favor of a square-pyramidal structure, once the radius of the central element is too large to allow for short tetrahedral metal−metal bonding.[3] According to the VSEPR model, T_d should here be more stable than C_{4v}. But actually, C_{4v} becomes more stable than T_d for heavier X.

In order to explain the transformation from T_d to C_{4v}, the optimized structures and relative energies for both symmetries of naked XAu_4^+ (X = N, P, As, Sb), and with phosphine ligands, $X(AuL)_4^+$, were determined by the Xα method. The structural parameters are given in Tables 2 and 3, and the corresponding energies are given in Table 4.

For the naked XAu_4^+ clusters, the energy is throughout lower for C_{4v}, and C_{4v} is strongly favored over T_d. For X = P, As, Sb and T_d symmetry, the Au···Au distances become expanded until the aurophilic interaction breaks down completely. In T_d there is no longer any aurophilic interaction. The $C_{4v} - T_d$ energy

TABLE 4: Relative Energies, $\Delta E = E(C_{4v}) - E(T_d)$ (E in kJ/mol) of XAu_4^+ and $X(AuPH_3)_4^+$ (X = N, P, As, Sb)

	NAu_4^+	PAu_4^+	$AsAu_4^+$	$SbAu_4^+$
ΔE	−29.09	−54.14	−143.65	−147.58
	$N(AuPH_3)_4^+$	$P(AuPH_3)_4^+$	$As(AuPH_3)_4^+$	$Sb(AuPH_3)_4^+$
ΔE	66.15	1.23	−43.65	−52.71

TABLE 5: Mulliken Populations and Charges of XAu_4^+ and $X(AuPH_3)_4^+$ (X = N, P, As, Sb)

system	sym.	Au6s	Au6p	Au5d	Au5f	Q_{Au}	Q_X	Q_{PH_3}
NAu_4^+	T_d	0.83	0.13	−0.47	0.02	0.49	−0.96	
	C_{4v}	0.83	0.22	−0.44	0.03	0.36	−0.44	
PAu_4^+	T_d	0.99	0.10	−0.41	0.01	0.31	−0.23	
	C_{4v}	0.94	0.23	−0.41	0.02	0.23	0.09	
$AsAu_4^+$	T_d	0.92	0.09	−0.34	0.01	0.32	−0.28	
	C_{4v}	0.89	0.21	−0.38	0.02	0.26	−0.04	
$SbAu_4^+$	T_d	0.93	0.08	−0.29	0.00	0.29	−0.14	
	C_{4v}	0.89	0.21	−0.36	0.02	0.24	0.04	
$N(AuPH_3)_4^+$	T_d	1.04	0.33	−0.63	0.03	0.23	−1.20	0.32
	C_{4v}	0.93	0.43	−0.62	0.04	0.22	−1.08	0.30
$P(AuPH_3)_4^+$	T_d	1.10	0.33	−0.52	0.02	0.08	−0.54	0.31
	C_{4v}	1.03	0.45	−0.52	0.03	0.02	−0.24	0.29
$As(AuPH_3)_4^+$	T_d	1.10	0.31	−0.50	0.02	0.07	−0.52	0.31
	C_{4v}	1.02	0.41	−0.52	0.02	0.07	−0.40	0.28
$Sb(AuPH_3)_4^+$	T_d	1.11	0.30	−0.45	0.01	0.03	−0.37	0.32
	C_{4v}	1.01	0.41	−0.49	0.02	0.05	−0.33	0.29

differences (−54.14, −143.65, and −147.58 kJ/mol) are estimates for the aurophilic interaction energies of PAu_4^+, $AsAu_4^+$, and $SbAu_4^+$, respectively. They are >14−36 kJ/mol per Au···Au. It seems that the aurophilic interaction energy increases when the Au atoms are bound to a less-electronegative atom.

For the clusters with phosphines, the T_d is lower in energy for $N(AuPH_3)_4^+$, while C_{4v} is definitely lower for $As(AuPH_3)_4^+$ and $Sb(AuPH_3)_4^+$. For $As(AuPH_3)_4^+$ and $Sb(AuPH_3)_4^+$, the Au···Au distances go beyond the range of aurophilic attraction for T_d structures. The aurophilic attraction energies from the $C_{4v} - T_d$ energy differences are 10−13 kJ/mol per Au···Au interaction.

The interesting case is $P(AuPH_3)_4^+$, where the $C_{4v} - T_d$ Xα-energy difference is only 1.23 kJ/mol. Vibrational frequencies of $P(AuPH_3)_4^+$ have been determined for both T_d and C_{4v}. Both constitute stable structures without imaginary frequencies.

Pyykkö et al. had predicted $P(AuPH_3)_4^+$ to prefer C_{4v}.[5,10] No experimental structures have been reported so far. In order to confirm this result, we have performed post-HF structure optimizations of $P(AuPH_3)_4^+$ with TURBOMOLE-5.6, using the higher quality basis sets TZVP, with 2f added on Au (exponents 1.19, 0.2). The energies are lower for T_d by 84 kJ/mol and 101 kJ/mol, at the MP2 and CC2/(MP2 structure) levels, respectively. Our MP2 results of $P(AuPH_3)_4^+$ differ from Pyykkö's, who possibly applied an earlier program version. We clearly predict $P(AuPH_3)_4^+$ to have a T_d ground state. The phosphine ligands are essential for both X = P and X = N preferring T_d. Concerning As and Sb, the C_{4v} symmetry is favored both with and without phosphines.

The effect of the phosphine ligands on the X−Au bond lengths is a slight elongation by 11 pm for T_d symmetry. When the structure is C_{4v}, the ligands increase the As−Au distance by 8 pm and the Sb−Au distance by 17 pm. The C_{4v} Au−X−Au angles are also increased, by 2−7°. The phosphine effects may be due to both electronic and steric effects.

3.2. Mulliken Populations and Charges of XAu_4^+ and $X(AuPH_3)_4^+$. A Mulliken population analysis does not yield reliable absolute values. Still, the relative trends are usually in agreement with those of other approaches. Mulliken charges are reported in Table 5. The effective Mulliken charges on the gold atoms of naked XAu_4^+ vary between +1/4 and +1/2. There are 1/4 to 1/2 holes in the Au5d shell, 0.8 to 1.0 electrons in Au6s, and 0.1 to 0.2 ones in Au6p. Concerning the phosphine-ligated $X(AuPH_3)_4^+$ systems, the PH_3 soft base transfers about 0.3 electronic charges onto the XAu_4^+ clusters. They increase the Au 6s and 6p populations by about 0.1 to 0.2 e, and reduce the 5d hole by 0.1e. Then the Au atoms carry negligibly small (positive) effective charges. Small effective charges on Au seem to enhance the Au(I)-Au(I) attraction.[11] The Mulliken population analysis shows very similar charges for both symmetries. Only in the ligated clusters, there is a little more Au6p and a little less Au6s for C_{4v} symmetry.

TABLE 6: Bond Energy E (in kJ/mol) Decomposition of $N(AuPH_3)_4^+$ and $As(AuPH_3)_4^+$ with C_{4v} and T_d Symmetries

	C_{4v}	T_d	Δ^f
	$N(AuPH_3)_4^+$		
$E_{Pauli}{}^a$	22151.14	21988.95	162.19
$E_{ele.}{}^b$	−7620.03	−7399.84	−220.19
$E_{ster}{}^c$	14531.12	14589.11	−57.99
$E_{orb}{}^d$	−22240.61	−22364.75	124.14
$E_{tot}{}^e$	−7709.50	−7775.65	66.15
	$As(AuPH_3)_4^+$		
$E_{Pauli}{}^a$	20714.69	20941.51	−226.82
$E_{ele.}{}^b$	−7222.79	−7122.36	−100.43
$E_{ster}{}^c$	13491.91	13819.15	−327.24
$E_{orb}{}^d$	−20972.65	−21256.27	283.62
$E_{tot}{}^e$	−7480.75	−7437.10	−43.65

[a] E_{Pauli}: Pauli repulsion [b] E_{ele}: electrostatic attraction. [c] E_{ster}: steric interaction is the sum of E_{Pauli} and E_{ele}. [d] E_{orb}: orbital relaxation energy. [e] E_{tot}: total bond energy. [f] Δ: respective energy differences between C_{4v} and T_d structures.

TABLE 7: "Aurophilic Interaction Energies" $\Delta E = E(C_{4v}) - E(T_d)$ (in kJ/mol) of XAu_4^+ and $X(AuPH_3)_4^+$ (X = N, P, As, Sb), and Au···Au Distance Changes $\Delta R_{Au\cdots Au} = R_{Au\cdots Au}(C_{4v}) - R_{Au\cdots Au}(T_d)$ (in pm)

	NAu_4^+	PAu_4^+	$AsAu_4^+$	$SbAu_4^+$
$\Delta R_{Au\cdots Au}$	−52.8	−83.9	−109.0	−137.0
ΔE	−29.09	−54.14	−143.65	−147.58
	$N(AuPH_3)_4^+$	$P(AuPH_3)_4^+$	$As(AuPH_3)_4^+$	$Sb(AuPH_3)_4^+$
$\Delta R_{Au\cdots Au}$	−46.0	−91.6	−108.0	−135.0
ΔE	66.15	0.53	−43.65	−52.71

3.3. Bond Energy Decomposition and Aurophilic Attraction vs Au···Au Distance. In order to better understand the aurophilic interactions, we have chosen $N(AuPH_3)_4^+$ and $As(AuPH_3)_4^+$ as two extreme examples for a more detailed investigation. The bond energy break-down is presented in Table 6.

The A−B bond formation process can be split into two steps. At first, the promolecular state (A + B) is introduced, in which fragments A and B are superposed at molecular A−B positions, but the fragment orbitals are unchanged. The A−B interaction energy at this step is called steric energy, E_{ster}. It consists of the attractive electrostatic overlap interaction, E_{ele}, and the kinetic energy increase of uncoupled electrons due to the Pauli principle (Pauli repulsion), E_{Pauli}. At the second step, the promolecular state is relaxed to the final molecular state. In this step, the occupied and virtual orbitals of A and B are mixed: electronic population is transferred from the occupied orbitals of one fragment to the virtual orbitals of the same (polarization) and the other fragments (charge transfer).

In both compounds, the electrostatic energies are more stabilizing for the more-compact C_{4v} structures (by −220 kJ/

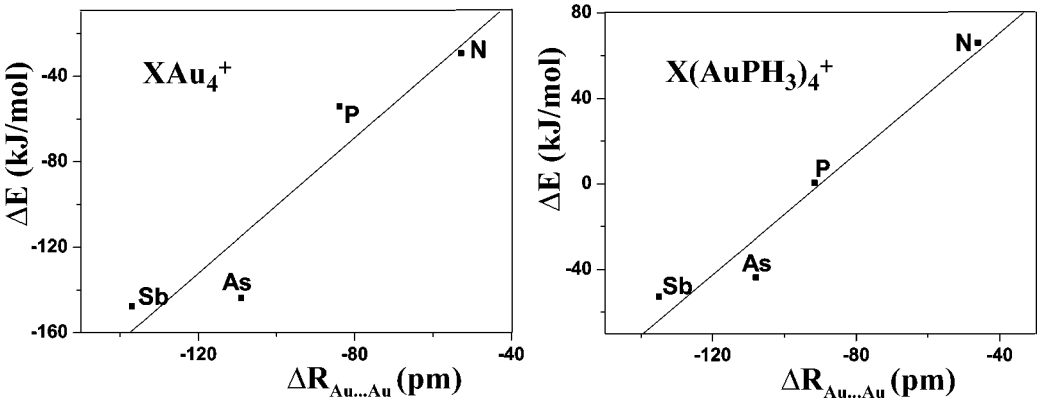

Figure 2. Energy vs Au···Au distance changes from T_d to C_{4v} structures of XAu_4^+ and $X(AuPH_3)_4^+$.

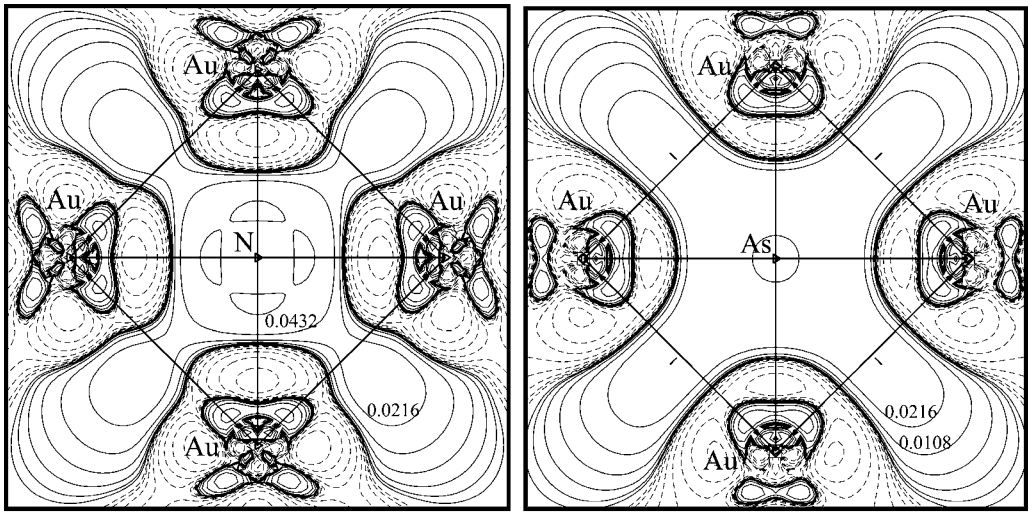

Figure 3. Electronic difference density $\Delta\rho$ (in e/Å^3) of (a) NAu_4^+, and (b) $AsAu_4^+$, both in C_{4v}, in the Au_4 plane (N, As above the plane!). Solid and dashed contour lines: increased and decreased electron density in the molecule.

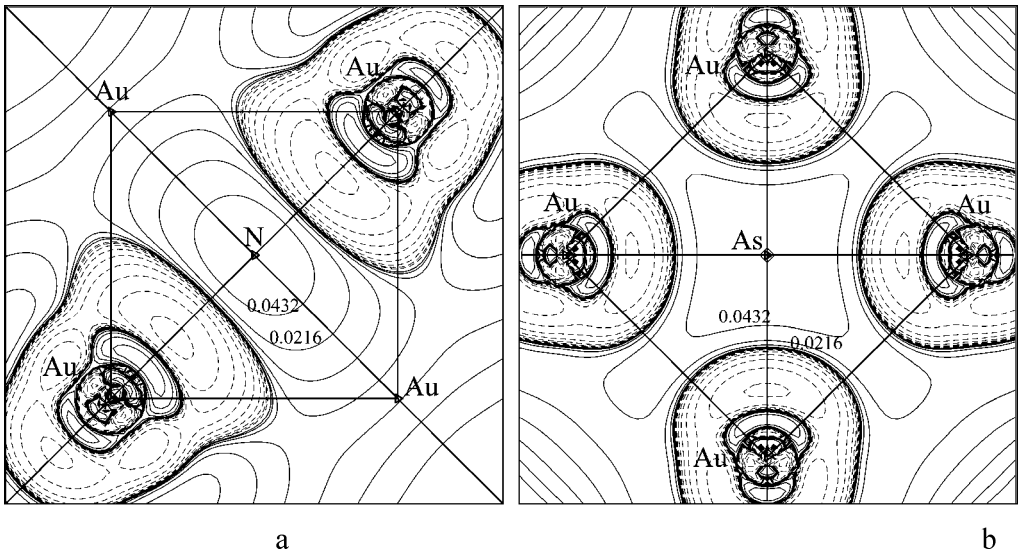

Figure 4. Electronic difference density $\Delta\rho$ (in e/Å^3) of (a) $N(AuPH_3)_4^+$, T_d structure, in an Au···Au plane, N and the other 2 Au above, and (b) $As(AuPH_3)_4^+$, C_{4v} structure, in the Au_4 plane, As above. Solid and dashed contour lines: increased and decreased electron density in the molecule.

mol for the N derivative, by −100 for the As one). The largest difference comes from the Pauli repulsion. It favors T_d for the N derivative (by 162 kJ/mol), but C_{4v} for the As one (by −227 kJ/mol). This trend is attenuated only somewhat by orbital relaxation, which favors T_d (by 124 kJ/mol for N, by 284 for As). $As(AuPH_3)_4^+$ adopts a C_{4v} structure, and $N(AuPH_3)_4^+$ adopts a T_d structure. $P(AuPH_3)_4^+$ forms the delicate intermediate case.

The energy differences between the T_d and C_{4v} structures are displayed versus the difference of Au···Au separations in

TABLE 8: Deviations ("Estimated Errors") $\bar{\Delta}$ of Calculated Molecular Aurophilic Distances $R_{Au\cdots Au}$ (in pm) from Experimental Crystallographic Estimates of $N(AuPH_3)_4^+$ (in T_d) and $As(AuPH_3)_4^+$ (in C_{4v})

	method								
	HF[a]	HF[b]	HF	MP2[a]	MP2[b]	MP2	Xα	VBP	B3LYP
$\overline{\Delta R}_{Au\cdots Au}$	+31	+38	+17	−10	+26	−9	0	+8	+15
$\overline{\lvert\Delta R_{Au\cdots Au}\rvert}$	+31	+38	+17	+15	+26	+9	0	+8	+15

[a] HF and MP2 structural values with big basis set from ref 9. [b] HF and MP2 structural values (ref 5) with small basis set.

Table 7 and Figure 2. The aurophilic interaction energy varies with 1.2 kJ/mol/pm of Au···Au distance for both XAu_4^+ and $X(AuPH_3)_4^+$.

3.4. Chemical Difference Densities. The electronic charge density distribution is a useful physical quantity that provides valuable information about the nature of bonding and nonbonding interactions. Relevant features come out in a better visible way, when the atomic ground-state densities are subtracted from the molecular density, $\Delta\rho = \rho_{mol} - \Sigma\rho_{atom.}$ We display the difference densities (at Xα level) of NAu_4^+, $AsAu_4^+$, and $As(AuPH_3)_4^+$ in C_{4v} and of $N(AuPH_3)_4^+$ in T_d structures in Figures 3 and 4 as typical examples.

Figure 3 displays about +0.03 e/Å^3 maximum density increase between the Au atoms in XAu_4^+ (C_{4v}). Similar values occur for $As(AuPH_3)_4^+$ (C_{4v}), see Figure 4b. We may take this as an indication of weak Au6sp valence orbital interference of covalent type. The chemical difference density of $N(AuPH_3)_4^+$ (T_d) in Figure 4a also shows positive values between the Au atoms, up to about +0.05 e/Å.[3]

The present standard DF approaches cannot account for electron correlation between non-overlapping fragments, that is, the long-range van der Waals attraction is missed. On the other hand, common DFs reasonably account for the correlation of overlapping fragments and reproduce standard covalent interactions. It seems that an overlap interference density increase of 1/20 to 1/40 e/Å^3 at overlapping densities of 0.2 to 0.5 e/Å^3 is already sufficient to obtain reasonable electron correlation energies. Then it would not simply be by accident than DFs yield reasonable aurophilic interaction energies.

4. Conclusions

In the present work, complexes of some central atom and Au ligands, $X(AuPH_3)_4^+$ (X = N, P, As, Sb), have been studied by means of some ab-initio (HF and post-HF) and DF methods. Our calculations reproduce the experimental T_d structure of $N(AuPH_3)_4^+$ and C_{4v} structure of $As(AuPH_3)_4^+$. T_d for $P(AuPH_3)_4^+$ and C_{4v} for $Sb(AuPH_3)_4^+$ are predicted. The present Xα geometric parameters for the molecules are in reasonable agreement with experimental crystal values (Table 8). Without the phosphine ligands, that is, XAu_4^+ and X = N, P, As, and Sb, a C_{4v} structure would always be preferred. The Au5d shell is not completely closed and may contribute in addition to Au6s and Au6p to the weak covalent metal−metal bonding that is also indicated by interference densities of up to 0.05 e/Å^3 between the interacting Au atoms.

Acknowledgment. We acknowledge the financial support by the National Nature Science Foundation of China (No. 20373041).

References and Notes

(1) Pyykkö, P. *Chem. Rev.* **1997**, *97*, 597.
(2) Scherbaum, F.; Grohmann, A.; Huber, B.; Krüger, C.; Schmidbaur, H. *Angew. Chem., Int. Ed. Engl.* **1988**, *27*, 1544; *Angew. Chem., Int. Ed. Engl.* **1988**, *100*, 1602.
(3) Zeller, E.; Beruda, H.; Kolb, A.; Bissinger, P.; Riede, J.; Schmidbaur, H. *Nature* **1991**, *352*, 141.
(4) Slovokhotov, Yu. L.; Struchkov, Yu. T. *J. Organomet. Chem.* **1984**, *277*, 143.
(5) Li, J.; Pyykkö, P. *Inorg. Chem.* **1993**, *32*, 2630.
(6) Pyykkö, P.; Runeberg, N.; Mendizabal, F. *Chem.*—Eur. J. **1997**, *3*, 1451.
(7) Pyykkö, P.; Mendizabal, F. *Chem.*—Eur. J. **1997**, *3*, 1458.
(8) Pyykkö, P.; Mendizabal, F. *Inorg. Chem.* **1998**, *37*, 3018.
(9) Andrae, D.; Haussermann, U.; Dolg, M.; Stoll, H.; Preuss, H. *Theor. Chim. Acta* (Berlin) **1990**, *77*, 123.
(10) Pyykkö, P.; Tamm, T. *Organometallics* **1998**, *17*, 4842.
(11) Wang, S. G.; Schwarz, W. H. E. *J. Am. Chem. Soc.* **2004**, *126*, 1266.
(12) Te Velde, G.; Bickelhaupt, F. M.; Baerends, E. J.; Guerra, C. F.; Van Gisbergen, S. J. A.; Snijders, J. G.; Ziegler, T. *J. Comput. Chem.* **2001**, *22*, 931.
(13) Ahlrichs, R.; Von Arnim, M. *Methods and Techniques in Computational Chemistry*: METECC-95; Clementi, E., Corongiu, G., Eds.; STEF: Cagliari, Italy, 1995; Chapter 13, p 509.
(14) Slater, J. C. *Phys. Rev.* **1951**, *81*, 385.
(15) Gaspar, R. *Acta Phys.* **1954**, *3*, 263.
(16) Schwarz, K. *Phys. Rev. B* **1972**, *5*, 2466.
(17) Vosko, S. H.; Wilk, L.; Nusair, M. *Can. J. Phys.* **1980**, *58*, 1200.
(18) Becke, A. D. *J. Chem. Phys.* **1988**, *88*, 2547.
(19) Perdew, J. P. *Phys. Rev. B* **1986**, *34*, 7406.
(20) Stephens, P. J.; Devlin, F. J.; Chabalowski, C. F.; Frisch, M. J. *J. Phys. Chem.* **1994**, *98*, 11623.
(21) Becke, A. D. *J. Chem. Phys.* **1993**, *98*, 5648.
(22) Te Velde, G.; Baerends, E. J. *J. Comput. Phys.* **1992**, *99*, 84.
(23) Lensch, C.; Jones, P. G.; Sheldrick, G. M. *Z. Naturforsch.* **1982**, *37b*, 944.
(24) Van Lenthe, E.; Ehlers, A. E.; Baerends, E. J. *J. Chem. Phys.* **1999**, *110*, 8943.
(25) Van Lenthe, E.; Baerends, E. J.; Snijders, J. G. *J. Chem. Phys.* **1994**, *101*, 9783.
(26) Van Lenthe, E.; Snijders, J. G.; Baerends, E. J. *J. Chem. Phys.* **1996**, *105*, 6505.
(27) Van Lenthe, E. *Int. J. Quantum Chem.* **1996**, *57*, 281.
(28) Häberlen, O. D.; Rösch, N. *J. Phys. Chem.* **1993**, *97*, 4970.
(29) O'Grady, E.; Kaltsoyannis, N. *Phys. Chem. Chem. Phys.* **2004**, *6*, 680.
(30) Riedel, S.; Pyykkö, P.; Mata, R. A.; Werner, H.-J. *Chem. Phys. Lett.* **2005**, *405*, 148.